0026-895X/09/7502-407–414$20.00
MOLECULAR PHARMACOLOGY
Vol. 75, No. 2
49981/3434986
Mol Pharmacol 75:407–414, 2009
Printed in U.S.A.

Expression and 1,4-Dihydropyridine-Binding Properties of Brain L-Type Calcium Channel Isoforms

Martina J. Sinnegger-Brauns, Irene G. Huber, Alexandra Koschak, Claudia Wild, Gerald J. Obermair, Ursula Einzinger, Jean-Charles Hoda,[1] Simone B. Sartori, and Jörg Striessnig

Department of Pharmacology and Toxicology, Institute of Pharmacy, and Center for Molecular Biosciences Innsbruck, University of Innsbruck, Innsbruck, Austria (M.J.S.-B., I.G.H., A.K., C.W., U.E., J.-C.H., S.B.S., J.S.); and Department of Physiology and Medical Physics, Medical University of Innsbruck, Innsbruck, Austria (G.J.O.)

Received June 30, 2008; accepted November 24, 2008

ABSTRACT

The L-type calcium channel (LTCC) isoforms $Ca_v1.2$ and $Ca_v1.3$ display similar 1,4-dihydropyridine (DHP) binding properties and are both expressed in mammalian brain. Recent work implicates $Ca_v1.3$ channels as interesting drug targets, but no isoform-selective modulators exist. It is also unknown to what extent $Ca_v1.1$ and $Ca_v1.4$ contribute to L-type-specific DHP binding activity in brain. To address this question and to determine whether DHPs can discriminate between $Ca_v1.2$ and $Ca_v1.3$ binding pockets, we combined radioreceptor assays and quantitative polymerase chain reaction (qPCR). We bred double mutants (Ca_v-DM) from mice expressing mutant $Ca_v1.2$ channels [*$Ca_v1.2DHP$*(−/−)] lacking high affinity for DHPs and from $Ca_v1.3$ knockouts [*$Ca_v1.3$*(−/−)]. (+)-[^{3}H]isradipine binding to *$Ca_v1.2DHP$*(−/−) and Ca_v-DM brains was reduced to 15.1 and 4.4% of wild type, respectively, indicating that $Ca_v1.3$ accounts for 10.7% of brain LTCCs. qPCR revealed that $Ca_v1.1$ and $Ca_v1.4$ α_1 subunits comprised 0.08% of the LTCC transcripts in mouse whole brain, suggesting that they cannot account for the residual binding. Instead, this could be explained by low-affinity binding (127-fold K_d increase) to the mutated $Ca_v1.2$ channels. Inhibition of (+)-[^{3}H]isradipine binding to *$Ca_v1.2DHP$*(−/−) (predominantly $Ca_v1.3$) and wild-type (predominantly $Ca_v1.2$) brain membranes by unlabeled DHPs revealed a 3- to 4-fold selectivity of nitrendipine and nifedipine for the $Ca_v1.2$ binding pocket, a finding further confirmed with heterologously expressed channels. This suggests that small differences in their binding pockets may allow development of isoform-selective modulators for LTCCs and that, because of their very low expression, $Ca_v1.1$ and $Ca_v1.4$ are unlikely to serve as drug targets to treat CNS diseases.

Depolarization-induced Ca^{2+} entry through voltage-gated Ca^{2+} channels controls a number of important physiological properties, including muscle contraction, cardiac pacemaking, hormone secretion, neurotransmitter release, and neuronal plasticity. Several subfamilies of voltage-gated Ca^{2+} channels with different pharmacological and biophysical properties evolved to serve these different physiological functions. Of these, the family of L-type Ca^{2+} channels (LTCCs) is characterized by high sensitivity to organic Ca^{2+} channel blockers (Catterall et al., 2005). Four LTCC isoforms exist, containing either $Ca_v1.1$, $Ca_v1.2$, $Ca_v1.3$, or $Ca_v1.4$ pore-forming α_1 subunits (Catterall et al., 2005). $Ca_v1.2$ and $Ca_v1.3$ LTCCs display very similar pharmacological properties, and they exhibit an overlapping expression pattern in the cardiovascular system, endocrine cells (e.g., pancreatic β-cells), and neurons (Hell et al., 1993; Sinnegger-Brauns et al., 2004). This has impeded distinction of their respective physiological roles. We have recently generated suitable mouse models to distinguish their contribution to different physiological processes. Whereas $Ca_v1.2$ channels regulate vascular tone and cardiac inotropy, $Ca_v1.3$ channels are crucial for pacemaking in sinoatrial node cells and atrioventricular conduction (Platzer et al., 2000; Sinnegger-Brauns et al., 2004). In mice, fast insulin secretion is closely coupled to $Ca_v1.2$ function (Schulla et al., 2003; Sinnegger-Brauns et al., 2004), whereas inner hair cell signaling and hearing depend on $Ca_v1.3$ (Platzer et al., 2000).

The central nervous system employs $Ca_v1.2$ channels for late-phase long-term potentiation in hippocampal neurons

This work was supported by the Austrian Research Fund [Grants P17159, P17807], the Tyrolean Research Fund, and the University of Innsbruck.
M.J.S.-B. and I.G.H. contributed equally to this work.
[1] Current affiliation: Department of Neuroscience, Faculty of Medicine, University of Geneva, Geneva, Switzerland.
Article, publication date, and citation information can be found at http://molpharm.aspetjournals.org.
doi:10.1124/mol.108.049981.

ABBREVIATIONS: LTCC, L-type Ca^{2+} channels; DHP, 1,4-dihydropyridine; qPCR, quantitative real-time PCR; WT, wild-type; ANOVA, analysis of variance.

and for spatial memory (Moosmang et al., 2005), whereas $Ca_v1.3$ channels, which can activate at more negative voltages (Platzer et al., 2000; Koschak et al., 2001; Lipscombe et al., 2004), seem to serve predominantly as modulators of neuronal spiking behavior and pacemaking (Olson et al., 2005; Chan et al., 2007).

$Ca_v1.3$-deficient mice lack amphetamine-sensitized locomotor activity (Giordano et al., 2006) and exhibit an antidepressant-like phenotype (Striessnig et al., 2006). $Ca_v1.3$ channels may also play an important pathophysiological role in Parkinson disease (Chan et al., 2007). Because presently available potent Ca^{2+} channel blockers such as the 1,4-dihydropyridines (DHPs) inhibit both $Ca_v1.2$ and $Ca_v1.3$ (Koschak et al., 2001; Helton et al., 2005), development of selective modulators of $Ca_v1.3$ channels would be required to determine whether they represent suitable targets to treat Parkinson disease, depression, and drug abuse. At present, it is unclear whether the highly conserved drug binding pockets (such as for the DHPs) of $Ca_v1.2$ and $Ca_v1.3$ channels offer enough structural heterogeneity to be exploited for that purpose. It also is still unresolved to what extent other LTCC isoforms ($Ca_v1.1$ and $Ca_v1.4$) can contribute to high-affinity drug binding in the central nervous system (Takahashi et al., 2003; Hemara-Wahanui et al., 2005) and could thus mediate pharmacological effects. These considerations raise two questions: 1) What are the expression levels of other LTCC isoforms ($Ca_v1.1$ and $Ca_v1.4$) in brain? 2) Does structural heterogeneity between the DHP binding pockets of $Ca_v1.2$ and $Ca_v1.3$ channels result in affinity differences that could be exploited for the development of isoform-selective modulators? This also raises a methodological issue, because although $Ca_v1.3$ channel complexes can be expressed for pharmacological analysis in mammalian cells, a native source of $Ca_v1.3$ channels is needed to validate data obtained with recombinant channels.

We employed a biochemical approach to address these questions, using a novel double-mutant mouse generated from previously established mouse models, radioligand binding assays, and extensive qPCR experiments.

Materials and Methods

Animals. The generation and detailed characterization of $Ca_v1.2$DHP(−/−) and $Ca_v1.3$(−/−) mice has been reported previously (Platzer et al., 2000; Sinnegger-Brauns et al., 2004). Double mutant *$Ca_v1.2DHP$*(−/−) × *$Ca_v1.3$*(−/−) mice were generated by crossing *$Ca_v1.3$*(−/−) male mice with *$Ca_v1.2DHP$*(−/−) female mice previously backcrossed into C57BL/6N background in five generations. Animals heterozygous for both mutant alleles were then crossed to obtain homozygous double mutants (referred to as Ca_v-DM). Tissues and RNA from 3- to 16-month old male mice or 3- to 12-month old male Sprague-Dawley rats were used for experiments. Animal handling was approved by the Bundesministerium für Bildung, Wissenschaft und Kultur (Vienna, Austria) in accordance with international laws and policies of animal welfare.

Recombinant α_1 cDNAs. The following α_1 subunit cDNAs were used (GenBank accession numbers given in parentheses): rabbit $Ca_v1.2$ (X15539), human $Ca_v1.3$ (EU63339; Koschak et al., 2001), and human $Ca_v1.4$ (variant of NM_005183; Koschak et al., 2003). Replacement of phenylalanine by tyrosine at position 1414 in the $Ca_v1.4$ α_1 subunit (numbering according to Koschak et al., 2003) to yield $Ca_v1.4_{F1414Y}$ followed published PCR procedures (Hoda et al., 2005), using an AgeI/EcoRI cassette. The mutation was confirmed by DNA sequencing (MWG Biotech, Ebersberg, Germany).

Transfection and Cell Culture. tsA201 cells were maintained in DMEM/F-12 medium (Invitrogen, Carlsbad, CA) enriched with 10% (v/v) fetal calf serum (SEBAK, Suben, Austria) and 2 mM L-glutamine and containing 44 mM $NaHCO_3$. Cells were incubated at 5% CO_2/37°C, plated on 10-cm culture dishes, and grown to approximately 70% confluence for transfection. α_1 subunits were transiently expressed together with $\alpha_2\delta_1$ (Genbank accession number NM_001082276) and β_{1a} (M25817) subunits in pcDNA3 (Invitrogen). Expression plasmids were combined at equimolar concentrations with a total subunit cDNA amount of 10.5 μg per 10-cm culture dish. Cells were transfected by calcium phosphate precipitation of DNA according to standard protocols. Medium was refreshed 8 to 12 h after transfection. Cells were harvested after two more days of incubation.

Membrane Preparation and Immunoblot Analysis. Microsomal membranes from brain tissue and tsA201 cells were prepared as described previously (Glossmann and Ferry, 1985; Reimer et al., 2000; Sinnegger-Brauns et al., 2004). Membrane protein concentrations were determined by Lowry or Bradford assays (Lowry et al., 1951; Bradford, 1976) with bovine serum albumin as a standard. Expression of recombinant proteins was monitored using Western Blot analysis as described previously (Hoda et al., 2005).

Radioreceptor Assay. (+)-[^{3}H]Isradipine (75–80 Ci/mmol) was purchased from PerkinElmer Life and Analytical Sciences (Vienna, Austria). Unlabeled racemic isradipine and (−)-isradipine were a gift from Novartis (Basel, Switzerland). (+)-Tetrandrine was a gift from MSD Sharp and Dohme (Rahway, NJ). (+)-*cis*-Diltiazem was from Gödecke (Freiburg, Germany). Mibefradil was provided by Roche (Basel, Switzerland). Azidopine was purchased from GE Healthcare (Chalfont St. Giles, Buckinghamshire, UK). Racemic nitrendipine and amlodipine as well as nifedipine were purchased from Sigma-Aldrich (Vienna, Austria). Stock solutions of all unlabeled drugs were prepared in dimethyl sulfoxide. Binding experiments were performed in binding buffer (50 mM Tris-HCl, pH 7.4, 0.1 mM phenylmethylsulfonyl fluoride, and 1 mM $CaCl_2$) in a final assay volume of 0.5 (brain microsomes) or 1 ml (tsA201 cell microsomes), respectively. Nonspecific binding was determined in the presence of 1 μM unlabeled isradipine. After incubation for 90 to 120 min at 22°C or 60 min at 37°C (binding stimulation) in a water bath, free ligand was removed by rapid filtration of the assay mixture over GF/C Whatman glass fiber filters (Sigma-Aldrich, Vienna, Austria), which had been pretreated with 0.25% (v/v) polyethylenimine for 30 min at 22°C. Filters were washed three times with ice-cold buffer (50 mM Tris-HCl, pH 7.4) and then counted for radioactivity to quantify bound ligand.

RNA Isolation and Reverse Transcription. Animals were euthanized by CO_2 exposure, and brains were excised after decapitation. Brain regions were dissected on ice with the help of a stereotaxic atlas (Franklin and Paxinos, 1997). Tissue was shock-frozen in liquid nitrogen and stored at −80 C until further processing. Total RNA was isolated using the RNAqueous-4PCR Kit (Ambion, Austin, TX; for brain tissues) or the E.Z.N.A. Total RNA Kit (Omega Bio-tek, Doraville, GA; for skeletal muscle and eye) according to the manufacturers' instructions. Total RNA was treated with DNase I (RNAqueous-4PCR Kit; Ambion), which effectively removed genomic contamination. RNA integrity was routinely checked for the presence of distinct 28S and 18S rRNA bands after loading 1 to 2 μg of RNA on a denaturating gel (formaldehyde SeaKem agarose gel, 1%). Total RNA (1 μg) was reverse-transcribed using RevertAid H Minus first-strand cDNA Synthesis Kit with random hexamer primers (MBI Fermentas, St. Leon-Rot, Germany). RNA and cDNA concentrations were determined photometrically.

Quantitative Real-Time PCR. The relative abundance of different LTCC transcripts was assessed by TaqMan quantitative PCR using a standard curve method as described previously (Koschak et al., 2007). Specific TaqMan Gene Expression Assays, designed to span exon-exon boundaries, were purchased from Applied Biosystems (Foster City, CA). The following primers (MWG Biotech) were

used for PCR amplification of assay-specific fragments using whole brain cDNA as a template. Mouse: $Ca_v1.1$: forward, 5′-GTTACATGAGCTGGATCACACAG-3′; reverse, 5′-ATGAGCATTTCGATGGTGAAG-3′. $Ca_v1.2$: forward, 5′-CATCACCAACTTCGACAACTTC-3′; reverse, 5′-CAGGTAGCCTTTGAGATCTTCTTC-3′. $Ca_v1.3$: forward, 5′-ACATTCTGAACATGGTCTTCACAG-3′; reverse, 5′-AGGACTTGATGAAGGTCCACAG-3′. $Ca_v1.4$: forward, 5′-CTCTTCATCTGTGGCAACTACATC-3′; reverse, 5′-GTACCACCTTCTCCTTGGGTACTA. Rat: $Ca_v1.1$: forward, 5′-CACACAGGGTAGCATGTAAGAGG-3′; reverse, 5′-TCGATACCCATAATATTCCTCCTG-3′. $Ca_v1.2$: forward, 5′-AAGACATAGACCCTGAGAATGAGG-3′; reverse, 5′-GAAGATCACCAGCCAGTAGAAGAC-3′. $Ca_v1.3$: forward, 5′-ATTAGGTCTGAGTCAGGAGACGAG-3′; reverse, 5′-TCGTCATCTTCTAAGAAACCTTGG-3′. $Ca_v1.4$: forward, 5′-TTCTACAGTTGCACTGATGAAGC-3′; reverse, 5′-AAGGCGATGATGATGATGTAGAC-3′. The integrity of the obtained fragments was confirmed by sequencing (MWG Biotech). Fragment concentrations were determined in a Wallac 1420 Multilabel Counter (PerkinElmer Life and Analytical Sciences) using the Quant-IT PicoGreen dsDNA Reagent (Invitrogen) according to the manufacturer's instructions, and standard curve dilutions were calculated subsequently. Four to five standard curves with 10-fold serial dilutions from 10^7 to 10 molecules of the respective fragment were generated for each assay. Assay efficiencies were calculated from the slope of the resulting average standard curve equation. Limits of quantification in the linear range of the individual standard curves were determined by calculating the relative S.D. of the replicate values obtained for each amount of fragment. The reliable quantification range was then defined by the fragment quanta at which measurements showed relative S.D. values of less than 1%. Assay IDs, their efficiency (E), and reliable quantification range (molecules) were as follows: Mouse: $Ca_v1.1$ α_1, Mm00489257_m1, E = 94.9%, 10^3 to 10^7; $Ca_v1.2$ α_1, Mm00437917_m1, E = 93.4%, 10^2 to 10^7; $Ca_v1.3$ α_1, Mm01209919_m1, E = 97.0%, 10^2 to 10^7; $Ca_v1.4$ α_1, Mm00490443_m1, E = 94.3%, 10^1 to 10^7. Rat: $Ca_v1.1$ α_1, customized (target base 2302 according to GenBank accession number L04684), E = 95.8%, 3×10^2 to 2×10^6; $Ca_v1.2$ α_1, Rn00709287_m1, E = 95.6%, 10^2 to 10^7; $Ca_v1.3$ α_1, Rn01453378_m1, E = 90.1%, 3×10^2 to 10^7; $Ca_v1.4$ α_1, Rn00586734_m1, E = 98.1%, 10^2 to 7×10^6.

qPCR was performed in triplicate measurements using 20 ng of total RNA equivalents of cDNA and the specific TaqMan Gene Expression Assay in a final volume of 20 μl in TaqMan Universal PCR Master Mix (Applied Biosystems). Samples were obtained from at least two independent reverse transcriptions of at least two independent RNA preparations from each species and strain examined (with the exception of muscle and eye controls, where only one reverse transcription of the respective preparations was performed). β-Actin transcript monitoring served to control the quality of RNA preparations and reverse transcriptions (mouse, Mm00607939_s1; rat, Rn01412977_g1). Samples containing RNA and samples without templates served as negative controls. Analysis was performed using the ABI PRISM 7500 Sequence Detector (Applied Biosystems). The relative abundance of each of the four different LTCC RNAs was expressed as the percentage of the sum of LTCC molecules per experiment.

Data Analysis and Statistics. Data were analyzed using Origin 6.1 (OriginLab Corp., Northampton, MA) and Prism 4.03 (GraphPad, San Diego, CA) employing the statistical tests indicated in the text and figure legends. P values <0.05 were considered statistically significant. Data are expressed as means ± S.E.M.—except where indicated otherwise—for the given number of experiments.

Results

Residual LTCC Binding Activity in *$Ca_v1.3$*(−/−)/*$Ca_v1.2DHP$*(−/−) Double Mutant Mice. We have previously shown that elimination of high DHP sensitivity of $Ca_v1.2$ channels in *$Ca_v1.2DHP$*(−/−) mutant mice reduced (+)-[^{3}H]isradipine binding activity to 15% of wild-type (WT) levels in brain (Sinnegger-Brauns et al., 2004). This residual activity was concluded to be associated with $Ca_v1.3$ channels, but the possibility of contribution by other LTCC isoforms has never been investigated. To quantify the contribution by LTCCs other than $Ca_v1.2$ and $Ca_v1.3$ to high-affinity DHP binding in mouse brain, we generated *$Ca_v1.3$*(−/−) × *$Ca_v1.2DHP$*(−/−) (Ca_v-DM) double mutant mice. In these mice, high-affinity DHP binding to $Ca_v1.2$ LTCCs is prevented by a missense mutation in $Ca_v1.2$ (Sinnegger-Brauns et al., 2004), and high-affinity binding to $Ca_v1.3$ is eliminated by $Ca_v1.3$ deficiency (Platzer et al., 2000). As a consequence, any residual binding in these mice should prompt a further biochemical analysis to determine a possible expression of other LTCCs. As expected, homozygous Ca_v-DM mice were viable and their phenotype was indistinguishable from that of *$Ca_v1.3$*(−/−) mice (Platzer et al., 2000).

In whole-brain microsomal membranes of *$Ca_v1.2DHP$*(−/−) mice, specific binding of the LTCC-selective high affinity probe (+)-[^{3}H]isradipine decreased to 15.1 ± 1.9% (mean ± S.E.M., $n = 5$) of WT values (Fig. 1A). A significant further reduction to 4.4 ± 0.5% ($p = 0.0006$, unpaired t test, $n = 5$) of WT values was observed in Ca_v-DM mice. Depending on experimental conditions [membrane protein concentration, presence of (+)-*cis*-diltiazem, see Fig. 1 and Table 1], this residual specific binding corresponded to 100 to 700 dpm and was reproducible in three individual preparations. These data demonstrate that more than 95% of LTCC-associated DHP binding in mouse brain occurs at $Ca_v1.2$ and $Ca_v1.3$, the latter participating in 10.7% of (+)-[^{3}H]isradipine binding activity.

To determine whether the remaining activity is linked to LTCCs or represents specific binding to other proteins, we further examined its properties. A hallmark of DHP interaction with LTCC α_1-subunits is the specific stimulation by the structurally unrelated benzothiazepine (+)-*cis*-diltiazem through a noncompetitive interaction mechanism (Brauns et al., 1997). As illustrated in Fig. 1B, 10 μM (+)-*cis*-diltiazem significantly enhanced (+)-[^{3}H]isradipine binding to Ca_v-DM brain membranes to 323 ± 31% ($n = 3$) of control. Furthermore, binding was abolished by 300 nM unlabeled racemic isradipine (corresponding to a 150 nM concentration of the active (+)-enantiomer), which indicates that the K_d of the residual binding was in the low nanomolar range. Based on

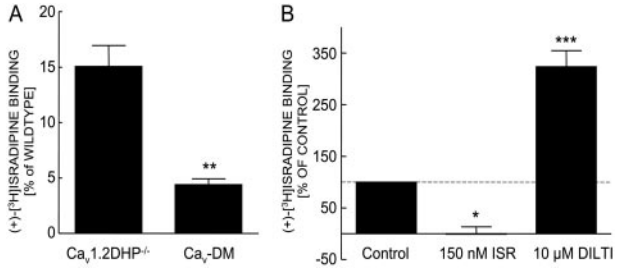

Fig. 1. Properties of (+)-[^{3}H]-isradipine binding to mouse brain membranes. A, residual binding in $Ca_v1.2$DHP(−/−) and Ca_v-DM brains was determined at radioligand concentrations (0.43 ± 0.07 nM, mean ± S.D., $n = 5$) known to cause high occupancy of high-affinity sites on $Ca_v1.2$ and $Ca_v1.3$ α_1 subunits; protein concentrations were 0.16 to 0.32 μg/ml protein. Data are means ± S.E.M. ($n = 5$). B, inhibition of (+)-[^{3}H]isradipine binding by 150 nM unlabeled (+)-isradipine (ISR, employed as 300 nM (±)-isradipine) and enhancement of (+)-[^{3}H]isradipine (0.5 nM) binding by 10 μM diltiazem (DILTI). Data are means ± S.E.M. ($n = 3$). Statistical difference from control is indicated (one-way ANOVA, Bonferroni post-test): *, $p < 0.05$; **, $p < 0.01$; ***, $p < 0.001$.

these characteristics, we conclude that the residual (+)-[^{3}H]isradipine binding in Ca_v-DM brains occurs at LTCCs and could therefore be associated with $Ca_v1.1$ and/or $Ca_v1.4$ channels. Alternatively, it could reflect residual (lower affinity) binding to the mutant $Ca_v1.2$ α_1 subunit.

Lack of High-Affinity DHP Binding to Recombinant $Ca_v1.4$ and $Ca_v1.4_{F1414Y}$ LTCCs. To distinguish between these possibilities, we first tested whether $Ca_v1.4$ channels can be detected in radioligand binding experiments. Expression of $Ca_v1.4$ together with auxiliary subunits in tsA201 cells did not yield specific, protein-concentration-dependent high-affinity (+)-[^{3}H]isradipine binding above background levels. Representative results obtained from three different membrane preparations are illustrated in Fig. 2B. Protein-concentration-dependent specific binding was also missing at higher (1.3–3 nM, $n = 3$) or lower ($n = 5$) (+)-[^{3}H]isradipine concentrations. Western blot experiments revealed that the absence of $Ca_v1.4$ binding activity was not due to a failure of transient $Ca_v1.4$ α_1 protein expression (Fig. 2A) (Koschak et al., 2003; Hoda et al., 2005). In comparison, membrane preparations from $Ca_v1.2$-transfected cells obtained in parallel experiments showed a robust signal with the expected binding densities (220 ± 31 fmol/mg of protein; Fig. 2B). Furthermore, specific binding could not be induced in the presence of 1, 3, and 10 μM concentrations of the nonDHP Ca^{2+} channel blockers (+)-*cis*-diltiazem, (+)-tetrandrine, and mibefradil (Table 1), which caused a robust stimulation of (+)-[^{3}H]isradipine binding to $Ca_v1.2$ (all three drugs) and $Ca_v1.3$ LTCCs [only tetrandrine and (+)-*cis*-diltiazem; see legend to Table 1] expressed under identical experimental conditions. In summary, our data suggest that, contrary to other LTCCs, the expression of $Ca_v1.4$ channels cannot be quantified using radioreceptor assays, despite their sensitivity to LTCC modulators in electrophysiological studies (Koschak et al., 2003). This could be due to a slightly higher K_d (which would reduce occupancy below levels detectable under our experimental conditions) and/or to very fast binding kinetics that cause dissociation of labeled channel complexes during filter washes. Alignment of the amino acid residues critical for DHP interaction in $Ca_v1.2$ α_1 subunits revealed that a tyrosine critical for DHP binding (present in $Ca_v1.1$, $Ca_v1.2$, and $Ca_v1.3$ α_1-subunits) is replaced by phenylalanine in $Ca_v1.4$ α_1 (Phe1414). We therefore generated the $Ca_v1.4$ mutant F1414Y to test whether a tyrosine at this position could restore high affinity binding. The exchange did not yield measurable specific DHP binding (Fig. 2B), despite efficient expression on the protein level (Fig. 2A). The failure of $Ca_v1.4$ detection by radioligand binding in our recombinant system implies that our DHP binding experiments with Ca_v-DM membranes do not permit predictions about $Ca_v1.4$ expression in mouse brain.

$Ca_v1.1$ and $Ca_v1.4$ RNA Transcripts Are Expressed at Very Low Levels in Mouse Brain. Because $Ca_v1.4$ quantification by radioligand binding was not feasible, we used qPCR to determine the relative magnitude of $Ca_v1.4$ and $Ca_v1.1$ α_1 transcript expression compared with $Ca_v1.2$ and $Ca_v1.3$ in both mouse and rat brain. In mouse, $Ca_v1.2$ was expressed at significantly ($p < 0.001$, $n = 9$; one-way ANOVA, Bonferroni post-test) higher densities than $Ca_v1.3$ in whole-brain preparations and all brain regions investigated (Fig. 3). $Ca_v1.3$ contributed 19.4 ± 1.6% (mean, ± S.E.M.) of total LTCC α_1-subunit transcripts in whole brain (Fig. 3; 7595 median number of molecules/20-ng RNA equivalent), in accordance with our biochemical estimate. The relative abundance of $Ca_v1.3$ transcripts was higher in rat than in mouse brain, where $Ca_v1.3$ significantly exceeded $Ca_v1.2$ α_1 RNA expression in all regions examined (Fig. 4).

$Ca_v1.4$ comprised 0.03 ± 0.01% of L-type transcripts in mouse whole brain, which corresponds to only 3 to 30 molecules/20-ng RNA equivalent. Although the $Ca_v1.4$ transcript number was within our quantification range (>10 molecules/20 ng; see *Materials and Methods*) in cerebral cortex and nucleus accumbens, the relative abundance and absolute

TABLE 1

Modulation of (+)-[^{3}H]-isradipine binding to recombinant $Ca_v1.4$, $Ca_v1.2$, and $Ca_v1.3$ LTCCs by the non-DHP calcium channel blockers (±)-tetrandrine, (+)-cis-diltiazem, and mibefradil

Ligand concentration was 0.14 nM. tsA201 cell membrane protein concentration was 50 to110 μg/ml. Specific binding is given in percentage of control (means ± S.E.M.). Note that mibefradil inhibits binding to $Ca_v1.3$ but acts stimulatory on $Ca_v1.2$.

Calcium Channel Blockers	1 μM	3 μM	10 μM	*n*
(±)-Tetrandrine				
$Ca_v1.4$	N.S.B.	N.S.B.	N.S.B.	2
$Ca_v1.2$	236 ± 21	277 ± 22	290 ± 18	3
$Ca_v1.3$	218 ± 9	248 ± 12	249 ± 9	6
(+)-*cis*-Diltiazem				
$Ca_v1.4$	N.S.B.	N.S.B.	N.S.B.	2
$Ca_v1.2$	116 ± 5	134 ± 6	171 ± 6	4
$Ca_v1.3$	136 ± 3	154 ± 5	179 ± 6	6
Mibefradil				
$Ca_v1.4$	N.S.B.	N.S.B.	N.S.B.	2
$Ca_v1.2$	93 ± 18	155 ± 5	164 ± 6	4
$Ca_v1.3$	42 ± 4	63 ± 2	71 ± 3	6

N.S.B., no specific binding was observed in the absence or presence of the indicated concentrations of (±)-tetrandrine, (+)-cis-diltiazem, and mibefradil in membrane preparations of two independent transfections.

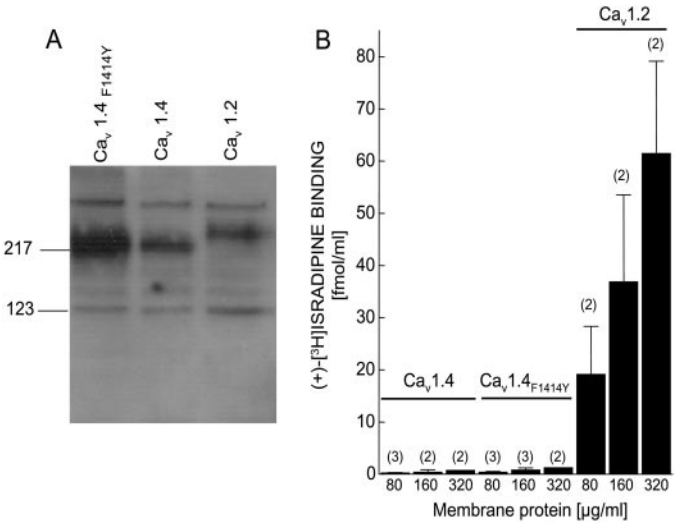

Fig. 2. A, transient expression of $Ca_v1.4$, $Ca_v1.4_{F1414Y}$, and $Ca_v1.2$ α_1 subunit proteins in tsA201 cells. Membrane proteins prepared from tsA201 cells transfected with wild-type $Ca_v1.4$ $\alpha1$ or $Ca_v1.4_{F1414Y}$ α_1 or $Ca_v1.2$ α_1 together with $\alpha_2\delta$ and β_{1a} and were separated (10 μg of membrane protein/lane) by SDS-PAGE and subjected to immunoblotting using a generic Ca_v1 α_1-subunit antibody (anti-$Ca_v1.1$–1382-1400, Hoda et al., 2005). Equal protein load per lane was confirmed by Coomassie staining of the membranes (not shown). B, equilibrium binding of (+)-[^{3}H]isradipine to recombinant $Ca_v1.4$ LTCCs. (+)-[^{3}H]isradipine (0.36–0.5 nM) was incubated (90 min 22°C) with the indicated concentration of membrane proteins prepared from tsA201 cells transfected as in A. One representative experiment obtained with membrane preparations from three different transfections for $Ca_v1.4$ and $Ca_v1.4_{F1414Y}$ is illustrated. Data are means ± S.E.M. Number of experiments is given in parentheses.

numbers were extremely low in these regions (cerebral cortex, 0.06 ± 0.02%, 20–120 copies/20 ng; nucleus accumbens, 0.03 ± 0.01%, 20–50 copies/20 ng).

Relative abundance (< 0.07%) and copy numbers (5–80, range in all brain regions) of $Ca_v1.4$ were similarly low in whole brain and all regions investigated in rat brain, where the assay was designed against a different region of the $Ca_v1.4$ gene (see *Materials and Methods*). However, up to 8600 copies/20 ng (rat) and 17,000 copies/20 ng (mouse) of $Ca_v1.4$ transcripts were detected in eye RNA preparations serving as positive controls (Figs. 3 and 4). This confirmed that our assay was able to efficiently detect $Ca_v1.4$ α_1-subunit RNA.

Like for $Ca_v1.4$, the relative abundance of $Ca_v1.1$ transcripts was also very low in mouse brain (0.05 ± 0.01% in whole brain), with the highest contribution in mouse cerebral cortex (0.12 ± 0.05%). Relative $Ca_v1.1$ expression was higher in the rat with transcript numbers within our quantification range (i.e., 300 copies/20 ng) in cortex (500–2700 copies/20 ng, 2.39 ± 0.36% of total LTCC α_1 transcripts) and nucleus accumbens (390–760 copies/20 ng, 0.62 ± 0.08%). As expected, $Ca_v1.1$ α_1 RNA was heavily expressed in skeletal muscle preparations (up to 390,000 copies/20 ng in mouse and 860,000 copies/20 ng in rat), which served as positive controls (Figs. 3 and 4).

It is noteworthy that the relative transcript abundance of $Ca_v1.1$ and $Ca_v1.4$ did not change in whole-brain preparations of *$Ca_v1.3$*(−/−) ($Ca_v1.4$, 0.07 ± 0.01%; $Ca_v1.1$, 0.06 ± 0.01%, $n = 13$) and *$Ca_v1.2DHP$*(−/−) ($Ca_v1.4$, 0.05 ± 0.003%; $Ca_v1.1$, 0.06 ± 0.003%, $n = 13$) mice, suggesting that the residual DHP binding in Ca_v-DM whole brain is unlikely to result from compensatory expression of $Ca_v1.1$ and/or $Ca_v1.4$.

Residual Binding Activity of $Ca_v1.2$. Our results suggested that neither $Ca_v1.1$ nor $Ca_v1.4$ is expressed at levels that could sufficiently support the residual LTCC-associated binding activity detected in homozygous Ca_v-DM mice. Therefore, the mutated $Ca_v1.2$ α_1 subunit resulting from their *$Ca_v1.2DHP$*(−/−) genotype remained as the most likely explanation for the residual binding. We estimated the lower affinity of the mutant $Ca_v1.2$ α_1 subunit as follows: for the experiments in Fig. 1A, we employed (+)-[^{3}H]isradipine concentrations (legend to Fig. 1) that cause similarly high occupancy of

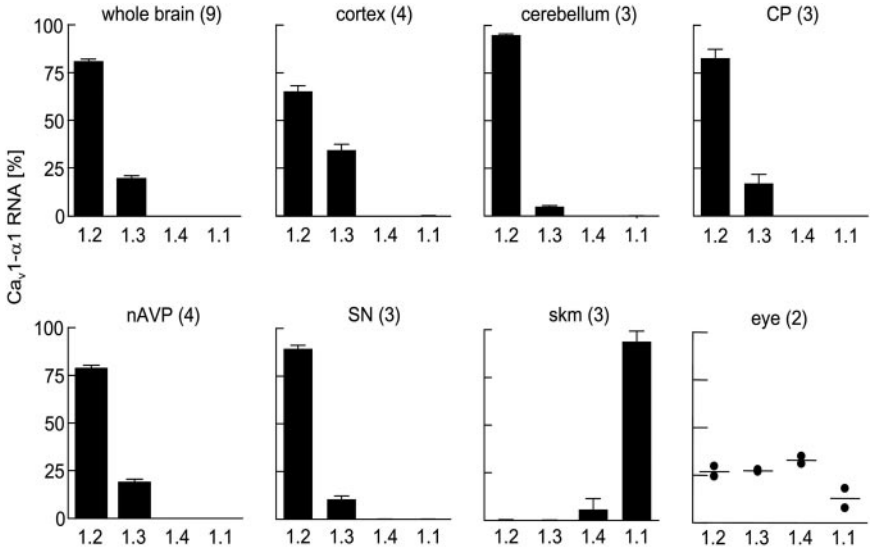

Fig. 3. Quantitative comparison of different LTCC isoform RNA transcripts in whole brain, brain regions, and control tissues of wild-type mice. qPCR assay results for $Ca_v1.1$ (1.1), $Ca_v1.2$ (1.2), $Ca_v1.3$ (1.3), and $Ca_v1.4$ (1.4) α_1 subunit RNA transcripts are given as percentage of total amount of all LTCC transcripts in each experiment. The number of experiments is given in parentheses. Means ± S.E.M. (individual data points for eye preparations) are illustrated. Relative expression levels of individual isoforms differed significantly from each other (not indicated; one-way ANOVA, Bonferroni post-test), except for comparisons between $Ca_v1.1$ and $Ca_v1.4$. CP, caudate putamen; nAVP, nucleus accumbens and ventral pallidum; SN, substantia nigra; skm, skeletal muscle.

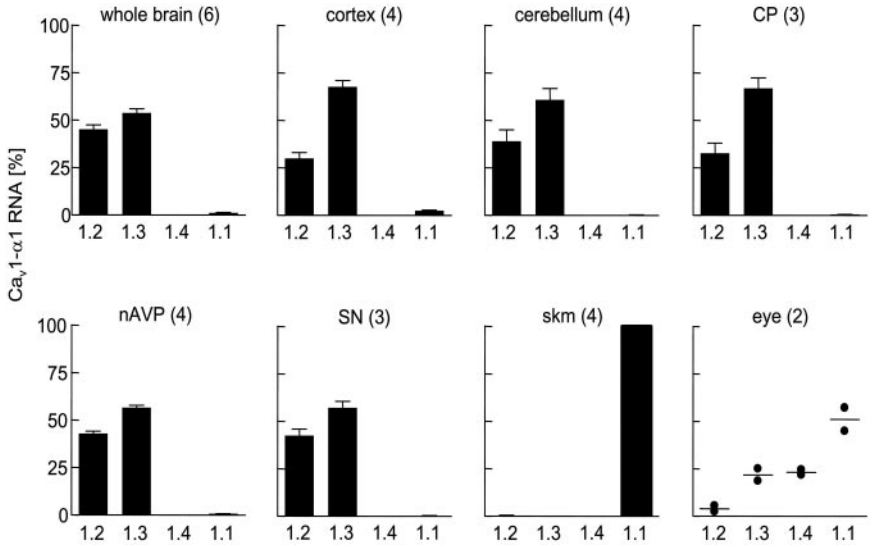

Fig. 4. Quantitative comparison of different LTCC isoform RNA transcripts in whole brain, brain regions, and control tissues of wild-type rats. qPCR assay results are illustrated as in Fig. 3. Relative expression levels of individual isoforms differed significantly from each other (not indicated; one-way ANOVA, Bonferroni post-test), except for comparisons between $Ca_v1.1$ and $Ca_v1.4$. Abbreviations are as in Fig. 3.

the high-affinity binding domains on both $Ca_v1.2$ and $Ca_v1.3$ LTCCs (Sinnegger-Brauns et al., 2004). From the difference in binding density between *$Ca_v1.2DHP$*(−/−) and Ca_v-DM mice, the contribution of $Ca_v1.3$ could be calculated as 10.7% of the total binding activity (see Fig. 1A). Assuming that only $Ca_v1.2$ contributes to the remaining activity, 89.3% of binding in wild-type brains should be associated with $Ca_v1.2$; 4.4% of binding were retained in the Ca_v-DM mice. If the latter represented lower affinity binding to the mutant $Ca_v1.2$ α_1 subunit, it would correspond to a 20.3-fold decrease in occupancy. The higher K_d (K_{d2}) accounting for this decrease can be estimated as $K_{d2} = ((K_{d1} + F) \cdot 20.3) - F$, where K_{d1} is the K_d for the wild-type $Ca_v1.2$ channel [0.078 nM as previously determined by us in mouse brain preparations under identical experimental conditions (Sinnegger-Brauns et al., 2004)] and F is the concentration of free ligand (essentially identical to total ligand, 0.43 nM; see legend to Fig. 1). The 20.3-fold decrease in occupancy therefore translates into a 127-fold increase in K_d from 0.078 nM for the wild-type $Ca_v1.2$ channel (Sinnegger-Brauns et al., 2004) to K_{d2} = 9.88 nM for the mutant channel. This calculation is in agreement with the approximately 150-fold decrease in affinity previously estimated from electrophysiological data (Sinnegger-Brauns et al., 2004).

Selectivity of Some DHP Ca^{2+} Channel Blockers for the $Ca_v1.2$ DHP Binding Domain. As concluded from our binding data from Ca_v-DM mouse brain, the majority (71%; 10.7% of 15.1% remaining binding activity) of the residual high-affinity (+)-[^{3}H]isradipine sites in the *$Ca_v1.2DHP$*(−/−) mutants is associated with $Ca_v1.3$. Therefore, *$Ca_v1.2DHP$*(−/−) brain membranes should be suitable to determine the affinity of competitive inhibitors for native $Ca_v1.3$ channels. In contrast, having excluded $Ca_v1.1$ and $Ca_v1.4$ as likely contributors to (+)-[^{3}H]isradipine binding, the majority (89.3%) of binding in WT brain membranes should occur at $Ca_v1.2$ and thus allow determination of drug binding affinities for native $Ca_v1.2$ channels. We therefore exploited the *$Ca_v1.2DHP$*(−/−) model to test whether structurally different DHPs can discriminate between the native $Ca_v1.2$ and $Ca_v1.3$ binding pockets. WT and *$Ca_v1.2DHP$*(−/−) brain membranes were labeled with (+)-[^{3}H]isradipine in the absence and presence of increasing concentrations of unlabeled DHPs. The resulting IC_{50} values were similar for (±)-isradipine [mostly reflecting activity of the more active (+)-enantiomer], its less active (−)-enantiomer [(−)-isradipine], amlodipine, and azidopine, but a 3- to 4-fold higher affinity was observed in WT brains for nifedipine and nitrendipine (Fig. 5, A and B; Table 2; both the means of IC_{50} values and the selectivity ratios were significantly different). This indicated that these compounds exhibit higher affinity for $Ca_v1.2$. To further confirm this finding, we repeated these experiments in membranes prepared from tsA201 cells transiently transfected with $Ca_v1.2$ and $Ca_v1.3$ α_1 subunits (Fig. 5, C and D; Table 3). Again, nitrendipine and nifedipine were 3- to 4-fold selective for $Ca_v1.2$. Selectivity (albeit weaker, 2-fold or less) of amlodipine, isradipine (selectivity ratio differences), and azidopine (mean IC_{50} difference) was observed also in the recombinant system (Table 3). Our data demonstrate that some DHPs bind to LTCCs in an isoform-selective manner.

Discussion

Our data provide novel biochemical and pharmacological information about neuronal LTCCs in mammalian brain. By generating the double mutant strain Ca_v-DM from *$Ca_v1.2DHP$*(−/−) and *$Ca_v1.3$*(−/−) mice, we demonstrated the existence of a residual (+)-[^{3}H]isradipine binding com-

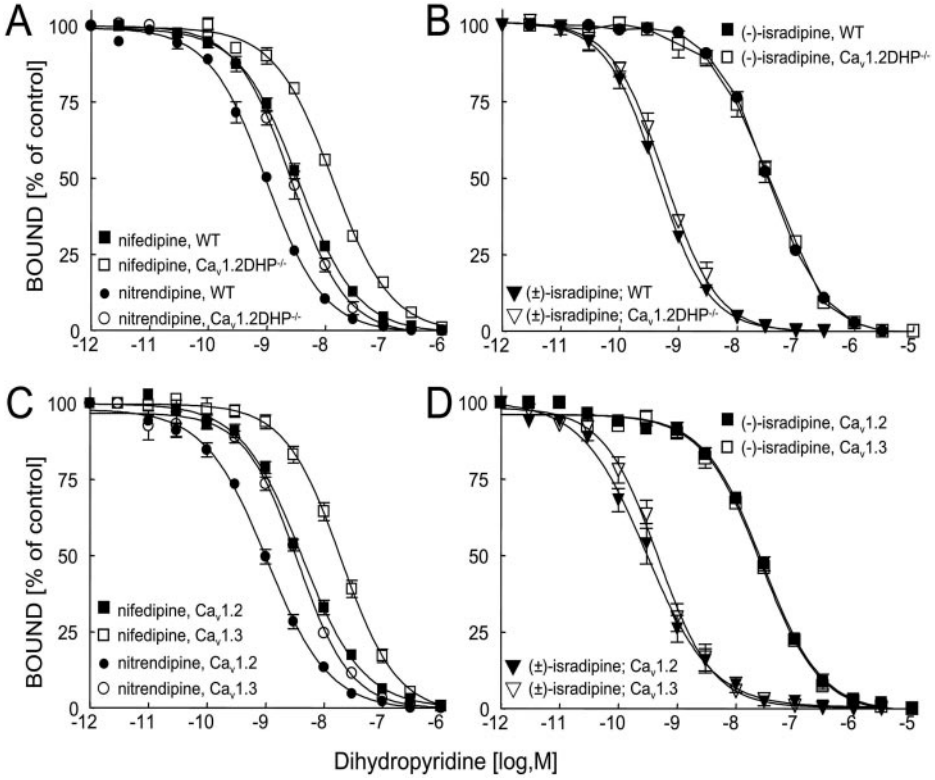

Fig. 5. Inhibition of (+)-[^{3}H]isradipine binding to native LTCCs in mouse brain membranes and to recombinant $Ca_v1.2$ and $Ca_v1.3$ LTCCs expressed in tsA201 cells by unlabeled DHPs. A and B, inhibition of (+)-[^{3}H]isradipine binding to native LTCCs in mouse brain membranes isolated from WT (filled symbols) or *$Ca_v1.2DHP$*(−/−) mice (open symbols) by the indicated DHPs. Radioligand concentrations were 0.14–0.18 nM; membrane protein concentrations were 0.3 mg/ml. Binding parameters and number of experiments are given in Table 2. Data are means ± S.E.M. C and D, inhibition of (+)-[^{3}H]isradipine binding to recombinant $Ca_v1.2$ and $Ca_v1.3$ LTCCs expressed in tsA201 cells together with $\alpha_2\delta_1$ and β_{1a} subunits by the indicated DHPs. Radioligand concentrations were 0.13–0.15 nM; membrane protein concentrations were 0.04 to 0.1 mg/ml. Binding parameters and number of experiments are given in Table 3. Data are means ± S.E.M.

ponent, which not only allowed us to obtain a more precise estimate for the contribution by the $Ca_v1.3$ channel (of approximately 11%) but also prompted us to investigate possible contribution by $Ca_v1.1$ and $Ca_v1.4$ LTCCs. Using qPCR, we show that $Ca_v1.1$ and $Ca_v1.4$ are expressed at very low levels and therefore cannot represent the residual binding component in mouse brain, which we instead explain by low-affinity binding to the mutated $Ca_v1.2$ subunit in *$Ca_v1.2DHP$(−/−)* mice. By excluding $Ca_v1.1$ and $Ca_v1.4$ as the relevant contributors to the residual binding component, we exploited *$Ca_v1.2DHP$(−/−)* mouse brains (predominant expression of $Ca_v1.3$) as an assay for native $Ca_v1.3$ channels. Our data demonstrate that some DHPs such as nifedipine and nitrendipine show substantial selectivity for $Ca_v1.2$ channels, which can explain some of the $Ca_v1.2$-selectivity observed also in functional experiments (Koschak et al., 2001; Helton et al., 2005).

We have previously obtained a higher estimate for the contribution of $Ca_v1.3$ channels to high affinity (+)-[^{3}H]isradipine binding activity (20–25%) using $Ca_v1.3$(−/−) mice (Clark et al., 2003) compared with the estimate obtained in this study. Although we found no evidence for changes of $Ca_v1.2\alpha1$ protein expression in $Ca_v1.3$(−/−) [and $Ca_v1.2$DHP(−/−)] mice in our previous analysis (Clark et al., 2003, Sinnegger-Brauns et al., 2004), we cannot rule out the possibility that a small decrease in $Ca_v1.2\alpha1$ protein expression resulted in an overestimation of $Ca_v1.3$ contribution in the knockouts. This again emphasizes the role of $Ca_v1.2$DHP(−/−) and Ca_v-DM mice as alternative models to obtain more precise estimates for the relative abundance of the $Ca_v1.3$ channel protein in mouse brain.

Our finding of very low $Ca_v1.1$ and $Ca_v1.4$ RNA expression levels is strengthened by the fact that we obtained the same result in two different species. However, our data stand in contrast to a study reporting relatively high levels of $Ca_v1.1$ expression in various human brain regions (Takahashi et al., 2003). In many of the brain regions investigated in that report, $Ca_v1.1$ transcript numbers were similar (such as in the putamen, occipital cortex, or spinal cord) or even exceeded those of $Ca_v1.3$, such as in the substantia nigra, pallidum, and caudate nucleus. We could not confirm such a high level of $Ca_v1.1$ expression in mouse and rat brain and different brain regions. In our study, the highest number of $Ca_v1.1$ transcripts was found in cerebral cortex and nucleus accumbens. In particular, we found no significant $Ca_v1.1$ expression in the caudate putamen of rat and mouse, the region reported to display the highest $Ca_v1.1$ expression level in human brain (Takahashi et al., 2003), and $Ca_v1.3$ expression by far exceeded $Ca_v1.1$ levels in all brain areas tested in our experiments. It is also noteworthy that we have observed a greater relative abundance of $Ca_v1.3$ in rat brain compared with mouse. Whether these differences represent species diversity or can be attributed to other confounding factors such as age, gender, or strain polymorphisms remains to be determined. Given the potential role of $Ca_v1.3$ LTCC activity for age-induced decreases in cognitive function (Veng et al., 2003, Herman et al., 1998) and the development of Parkinson disease (Chan et al., 2007), our finding deserves more detailed analysis in further experiments.

We found that one of the most sensitive detection methods, reversible labeling with (+)-[^{3}H]isradipine, failed to detect $Ca_v1.4$ LTCCs after expression in tsA201 cells under conditions that reliably yield $Ca_v1.4$ α_1 protein in Western blots, give rise to $Ca_v1.4$-mediated currents (Koschak et al., 2003; Hoda et al., 2005) and allow robust detection of recombinant $Ca_v1.2$ and $Ca_v1.3$ LTCCs by this radioligand (Fig. 2, Tables 1 and 3). We show that this is not due to the phenylalanine substitution of a tyrosine in position 1414 in the $Ca_v1.4$ α_1 subunit, a residue contributing to the DHP sensitivity of other LTCCs and present in all other LTCC $\alpha1$ subunits. In $Ca_v1.1$ channels, replacement of the homologous tyrosine by a phenylalanine results in an about 3-fold increase in the K_d for (+)-[^{3}H]isradipine (Peterson et al., 1996). Substituting $Ca_v1.4$ Phe1414 by tyrosine did not result in detectable bind-

TABLE 2

Affinities of different DHPs for brain membranes of *$Ca_v1.2DHP$(−/−)* and wild-type mice

Ligand concentration was 0.14–0.18 nM. Membrane protein concentration was 0.3 mg/ml. Data are given as means ± S.D. for the indicated number of experiments. Statistical significance of selectivity was determined from a direct comparison of IC_{50} values and from the selectivity ratios (WT:MUT) calculated from individual experiments carried out in parallel for both genotypes.

Dihydropyridine	WT	$Ca_v1.2$DHP(−/−)	IC_{50} WT:MUT	*n*
(±)-Isradipine				
IC_{50} (nM)	0.43 ± 0.03	0.59 ± 0.12	0.76 ± 0.20	3
Slope factor	0.99 ± 0.10	0.98 ± 0.08		
Azidopine				
IC_{50} (nM)	1.23 ± 0.71	1.08 ± 0.56	1.13 ± 0.18	3
Slope factor	0.94 ± 0.04	0.95 ± 0.04		
Nitrendipine				
IC_{50} (nM)	0.97 ± 0.11	2.79 ± 0.80^{+++}	0.37 ± 0.11**	4
Slope factor	0.89 ± 0.08	0.96 ± 0.10		
Nifedipine				
IC_{50} (nM)	3.42 ± 0.55	13.21 ± 1.05^{+++}	0.26 ± 0.06**	3
Slope factor	0.85 ± 0.04	0.87 ± 0.11		
(−)-Isradipine				
IC_{50} (nM)	35.2 ± 7.4	35.5 ± 5.2	0.98 ± 0.09	3
Slope factor	0.95 ± 0.01	0.86 ± 0.07		
Amlodipine				
IC_{50} (nM)	41.1 ± 1.2	39.2 ± 4.6	1.06 ± 0.14	3
Slope factor	0.93 ± 0.04	1.01 ± 0.02		

$^{+++}$ $P < 0.001$; unpaired student's *t* test.
** $P < 0.01$, for difference from unity, one-sample *t* test.

TABLE 3

Affinities of different DHPs for recombinant $Ca_v1.3$ and $Ca_v1.2$ channels

Ligand concentration was 0.13 to 0.15 nM. Membrane protein concentration was 40 to 100 μg/ml. Data are given as means ± S.D. for $n = 5$. Statistical significance of selectivity was obtained as described in Table 2. Selectivity ratios (WT:MUT) were calculated from individual experiments carried out in parallel for both channel isoforms.

Dihydropyridine	$Ca_v1.2$	$Ca_v1.3$	IC_{50} WT:MUT
(±)-Isradipine			
IC_{50} (nM)	0.40 ± 0.21	0.51 ± 0.20	0.76 ± 0.18*
Slope factor	0.80 ± 0.04	0.96 ± 0.12	
Azidopine			
IC_{50} (nM)	0.46 ± 0.10	0.65 ± 0.11^{+}	0.74 ± 0.23
Slope factor	0.85 ± 0.06	1.00 ± 0.11	
Nitrendipine			
IC_{50} (nM)	1.08 ± 0.27	3.59 ± 0.66^{+++}	0.31 ± 0.11***
Slope factor	0.82 ± 0.10	0.96 ± 0.12	
Nifedipine			
IC_{50} (nM)	4.45 ± 1.21	20.1 ± 4.78^{+++}	0.22 ± 0.04***
Slope factor	0.84 ± 0.12	0.92 ± 0.10	
(−)-Isradipine			
IC_{50} (nM)	29.7 ± 5.56	27.2 ± 3.67	1.09 ± 0.11
Slope factor	0.88 ± 0.13	0.86 ± 0.12	
Amlodipine			
IC_{50} (nM)	28.4 ± 11.8	60.1 ± 28.3	0.48 ± 0.11***
Slope factor	0.87 ± 0.11	0.94 ± 0.09	

$^{+}$ $P < 0.05$.
$^{+++}$ $P < 0.001$.
* $P < 0.05$.
*** $P < 0.001$.

ing activity. It is noteworthy that there are also some other amino acid exchanges in the putative $Ca_v1.4$ DHP binding pocket that could cause a reduction in (+)-[^{3}H]isradipine binding affinity (including proline-1037 and alanine-1087 in the IIIS5-IIIS6 pore loop). This may shift the K_d outside the detection range of our binding assay. A slightly lower affinity for the DHP binding pocket may also contribute to the lower sensitivity of $Ca_v1.4$ channel currents for isradipine compared with $Ca_v1.3$ and $Ca_v1.2$ (Koschak et al., 2003).

We demonstrated that nitrendipine and nifedipine exhibited 3- to 4- fold higher affinities for the $Ca_v1.2$ DHP binding pocket in the native membrane environment, a finding that was further confirmed employing recombinant channels. This represents the first comparison of the pharmacological properties of the DHP binding domains of native and recombinant $Ca_v1.2$ and $Ca_v1.3$ LTCC complexes. Nitrendipine and nifedipine are distinguished from the other DHPs tested by their NO_2 substituent at the 3′ and 2′ position of the phenyl ring, respectively. The existence of $Ca_v1.2$ selectivity was surprising given the very high sequence similarity within the DHP binding pocket of $Ca_v1.2$ and $Ca_v1.3$. Our findings indicate that nitrendipine and nifedipine can sense differences in the molecular architectures of these two binding domains. It therefore seems likely that such differences may also allow development of molecules with higher affinity for the $Ca_v1.3$ binding pocket. This could aid in the development of $Ca_v1.3$ selective LTCC blockers, which, based on emerging knowledge about the physiological role of $Ca_v1.3$ channels (Platzer et al., 2000; Striessnig et al., 2006; Chan et al., 2007), could open novel therapeutic strategies for the treatment of depression and Parkinson disease.

Acknowledgments

We thank G. Pelster and S. Haßler for expert technical assistance, L. Glatzl and C. Bachmann for animal care, Bettina Schlick for help with qPCR, and Bernhard E. Flucher for helpful discussions.

References

Bradford MM (1976) A rapid and sensitive method for the quantitation of microgram quantities of protein utilizing the principle of protein-dye binding. *Anal Biochem* **72:**248–254.

Brauns T, Prinz H, Kimball SD, Haugland RP, Striessnig J, and Glossmann H (1997) L-type calcium channels: binding domains for dihydropyridines and benzothiazepines are located in close proximity to each other. *Biochemistry* **36:**3625–3631.

Catterall WA, Perez-Reyes E, Snutch TP, and Striessnig J (2005) International Union of Pharmacology. XLVIII. Nomenclature and structure-function relationships of voltage-gated calcium channels. *Pharmacol Rev* **57:**411–425.

Chan CS, Guzman JN, Ilijic E, Mercer JN, Rick C, Tkatch T, Meredith GE, and Surmeier DJ. (2007) Rejuvenation' protects neurons in mouse models of Parkinson disease. *Nature* **447:**1081–1086.

Clark NC, Nagano N, Kuenzi FM, Jarolimek W, Huber I, Walter D, Wietzorrek G, Boyce S, Kullmann DM, Striessnig J, et al. (2003) Neurological phenotype and synaptic function in mice lacking the $Ca_v1.3$ alpha subunit of neuronal L-type voltage-dependent Ca^{2+} channels. *Neuroscience* **120:**435–442.

Franklin KBJ and Paxinos G (1997) *The Mouse Brain in Stereotaxic Coordinates*, Academic Press, London.

Giordano TP 3rd, Satpute SS, Striessnig J, Kosofsky BE, and Rajadhyaksha AM (2006) Up-regulation of dopamine D2L mRNA levels in the ventral tegmental area and dorsal striatum of amphetamine-sensitized C57BL/6 mice: role of $Ca_v1.3$ L-type Ca^{2+} channels. *J Neurochem* **99:**1197–1206.

Glossmann H and Ferry DR (1985) Assay for calcium channels. *Methods Enzymol* **109:**513–550.

Hell JW, Westenbroek RE, Warner C, Ahlijanian MK, Prystay W, Gilbert MM, Snutch TP, and Catterall WA (1993) Identification and differential subcellular localization of the neuronal class C and Class D L-type calcium channel a1 subunits. *J Cell Biol* **123:**949–962.

Helton TD, Xu W, and Lipscombe D (2005) Neuronal L-type calcium channels open quickly and are inhibited slowly. *J Neurosci* **25:**10247–10251.

Hemara-Wahanui A, Berjukow S, Hope CI, Dearden PK, Wu SB, Wilson-Wheeler J, Sharp DM, Lundon-Treweek P, Clover GM, Hoda JC, et al. (2005) A CACNA1F mutation identified in an X-linked retinal disorder shifts the voltage dependence of $Ca_v1.4$ channel activation. *Proc Natl Acad Sci U S A* **102:**7553–7558.

Herman JP, Chen KC, Booze R, and Landfield PW (1998) Up-regulation of alpha1D Ca^{2+} channel subunit mRNA expression in the hippocampus of aged F344 rats. *Neurobiol Aging* **19:**581–587.

Hoda JC, Zaghetto F, Koschak A, and Striessnig J (2005) Congenital stationary night blindness type 2 mutations S229P, G369D, L1068P, and W1440X alter channel gating or functional expression of $Ca_v1.4$ L-type Ca^{2+} channels. *J Neurosci* **25:**252–259.

Koschak A, Obermair GJ, Pivotto F, Sinnegger-Brauns MJ, Striessnig J, and Pietrobon D (2007) Molecular nature of anomalous L-type calcium channels in mouse cerebellar granule cells. *J Neurosci* **27:**3855–3863.

Koschak A, Reimer D, Huber I, Grabner M, Glossmann H, Engel J, and Striessnig J (2001) α1D ($Ca_v1.3$) subunits can form L-type Ca^{2+} channels activating at negative voltages. *J Biol Chem* **276:**22100–22106.

Koschak A, Reimer D, Walter D, Hoda JC, Heinzle T, Grabner M, and Striessnig J (2003) $Ca_v1.4\alpha1$ subunits can form slowly inactivating dihydropyridine-sensitive L-type Ca^{2+} channels lacking Ca^{2+}-dependent inactivation. *J Neurosci* **23:**6041–6049.

Lipscombe D, Helton TD, and Xu W (2004) L-type calcium channels: the low down. *J Neurophysiol* **92:**2633–2641.

Lowry OH, Rosebrough NJ, Farr AL, and Randall RJ (1951) Protein measurement with the folin phenol reagent. *J Biol Chem* **193:**265–275.

Moosmang S, Haider N, Klugbauer N, Adelsberger H, Langwieser N, Müller J, Stiess M, Marais E, Schulla V, Lacinova L, et al. (2005) Role of hippocampal $Ca_v1.2$ Ca^{2+} channels in NMDA receptor-independent synaptic plasticity and spatial memory. *J Neurosci* **25:**9883–9892.

Olson PA, Tkatch T, Hernandez-Lopez S, Ulrich S, Ilijic E, Mugnaini E, Zhang H, Bezprozvanny I, and Surmeier DJ (2005) G-protein-coupled receptor modulation of striatal $Ca_v1.3$ L-type Ca^{2+} channels is dependent on a Shank-binding domain. *J Neurosci* **25:**1050–1062.

Peterson BZ, Tanada TN, and Catterall WA (1996) Molecular determinants of high affinity dihydropyridine binding in L-type calcium channels. *J Biol Chem* **271:**5293–5296.

Platzer J, Engel J, Schrott-Fischer A, Stephan K, Bova S, Chen H, Zheng H, and Striessnig J (2000) Congenital deafness and sinoatrial node dysfunction in mice lacking class D L-type Ca^{2+} channels. *Cell* **102:**89–97.

Reimer D, Huber IG, Garcia ML, Haase H, and Striessnig J (2000) beta subunit heterogeneity of L-type Ca^{2+} channels in smooth muscle tissues. *FEBS Lett* **467:**65–69.

Schulla V, Renström E, Feil R, Feil S, Franklin I, Gjinovci A, Jing XJ, Laux D, Lundquist I, Magnuson MA, et al. (2003) Impaired insulin secretion and glucose tolerance in beta cell-selective $Ca_V1.2$ Ca^{2+} channel null mice. *EMBO J* **22:**3844–3854.

Sinnegger-Brauns MJ, Hetzenauer A, Huber IG, Renström E, Wietzorrek G, Berjukov S, Cavalli M, Walter D, Koschak A, Waldschütz R, et al. (2004) Isoform-specific regulation of mood behavior and pancreatic beta cell and cardiovascular function by L-type Ca^{2+} channels. *J Clin Invest* **113:**1430–1439.

Striessnig J, Koschak A, Sinnegger-Brauns MJ, Hetzenauer A, Nguyen NK, Busquet P, Pelster G, and Singewald N (2006) Role of voltage-gated L-type Ca^{2+} channel isoforms for brain function. *Biochem Soc Trans* **34:**903–909.

Takahashi Y, Jeong SY, Ogata K, Goto J, Hashida H, Isahara K, Uchiyama Y, and Kanazawa I (2003) Human skeletal muscle calcium channel alpha1S is expressed in the basal ganglia: distinctive expression pattern among L-type Ca^{2+} channels. *Neurosci Res* **45:**129–137.

Veng LM, Mesches MH, and Browning MD (2003) Age-related working memory impairment is correlated with increases in the L-type calcium channel protein alpha1D ($Ca_v1.3$) in area CA1 of the hippocampus and both are ameliorated by chronic nimodipine treatment. *Brain Res Mol Brain Res* **110:**193–202.

Address correspondence to: Jörg Striessnig, Department of Pharmacology and Toxicology, Institute of Pharmacy, and Center for Molecular Biosciences Innsbruck, University of Innsbruck, Peter-Mayr-Str. 1/I, A-6020 Innsbruck, Austria. E-mail: joerg.striessnig@uibk.ac.at